Decoupling Technique and Crosstalk Analysis for Coupled *RLC* Interconnects

Junmou Zhang and Eby G. Friedman

Department of Electrical and Computer Engineering
University of Rochester
Rochester, New York 14627–0231

***Abstract*— With lower wire resistance and faster signal rise times, the on-chip inductance plays an important role in determining the circuit performance and signal integrity characteristics. The self and mutual inductance must be considered in the analysis of crosstalk noise between coupled *RLC* interconnects. Based on the ABCD parameter matrix, a decoupling technique for two coupled identical *RLC* interconnects is developed. The inductances (capacitances) of two decoupled interconnects are the effective inductances (capacitances) when both inputs switch in the same and inverse direction, respectively. A model of the peak crosstalk noise is developed based on this decoupling technique, with the peak noise occurring at the time of flight t_{fmax} or $3t_{fmax}$. The model exhibits an average error of 6.8% as compared to SPICE. The peak crosstalk noise does not necessarily increase with greater coupling inductance or capacitance. The decoupling technique is further extended to two non-identical coupled interconnects, providing an upper limit on the peak crosstalk noise.**

I. Introduction

It is well accepted that the on-chip interconnect plays an important role in the performance and signal integrity of deep submicrometer VLSI circuits. With faster rise times and lower resistance, long wide wires in the upper metal layers exhibit significant inductive effects. An efficient *RLC* model of the on-chip interconnect is therefore critical to interconnect optimization in high level design, logic synthesis, and physical design.

Interconnect optimization that considers only one distributed *RLC* line is studied in [1], where the coupling effects from neighboring wires are ignored. Due to increased vertical/lateral aspect ratios of the interconnect and decreased interconnect spacing, the coupling (fringing) capacitance between interconnects approaches or is greater than the line-to-ground capacitance. Furthermore, coupling inductance occurs in both neighboring and non-neighboring wires. Ignoring these coupling capacitances and inductances will severely underestimate the interconnect delay and crosstalk noise between coupled interconnects.

A closed-form expression for the crosstalk noise between two identical *RLC* lines is developed in [2], assuming that the two interconnects are loosely coupled ($\frac{L_m}{L}\frac{C_c}{C} < 0.1$). In [3], a delay and crosstalk model is developed based on an effective inductance. This model, however, requires knowledge of the current return path and an empirical fitting parameter. In [4], a time domain expression for the output of coupled *RLC* interconnects is developed without explicitly requiring the Laplace transform of the transfer function. Delay and crosstalk noise expressions, however, ignore the effect of the capacitive load at the receiver end, and the peak crosstalk noise is assumed to occur at the time of flight t_f. In [5], a technique to decouple coupled *RLC* interconnects into independent interconnects is developed based on a modal analysis. This decoupling method, however, assumes a TEM mode approximation ($LC = \frac{1}{\mu\epsilon}$) which is only valid in a 2-D structure with a perfect current return path in the ground plane directly beneath the conductors [6].

Based on the ABCD parameter matrix, a technique to decouple two coupled lossy *RLC* interconnects into two independent interconnects is developed here without any assumptions. With this decoupling technique, an accurate crosstalk noise model for two identical coupled interconnects is developed, followed by a model of the maximum peak crosstalk noise between two non-identical coupled *RLC* interconnects. The model of the peak crosstalk noise exhibits an average error of 6.8% as compared to SPICE.

The rest of the paper is organized as follows. In Section II, a technique for decoupling two identical coupled *RLC* interconnects is developed. Based on this decoupling technique, a model of the peak crosstalk noise between two coupled interconnects is developed and compared to SPICE and other peak crosstalk noise models in Section III. In Section IV, a model of the maximum peak crosstalk noise between two non-identical coupled *RLC* interconnect is developed. Some conclusions are offered in Section V.

II. Decoupling Technique

Two identical coupled interconnects with a coupling capacitance c_c, mutual inductance l_m, ground capacitance c_g, self inductance l per unit length, and length h are shown in Fig. 1. The *Kirchhoff* equation for an infinitesimally small segment of these two coupled interconnects is given by

$$\Psi_i = E\Psi_o, \tag{1}$$

where $\Psi_i = [V_{i1}, V_{i2}, I_{i1}, I_{i2}]^T$, $\Psi_o = [V_{o1}, V_{o2}, I_{o1}, I_{o2}]^T$, and

$$E = \begin{bmatrix} 1 & 0 & (r+sl)dx & sl_m dx \\ 0 & 1 & sl_m dx & (r+sl)dx \\ s(c_g+c_c)dx & -sc_c dx & 1 & 0 \\ -sc_c dx & s(c_g+c_c)dx & 0 & 1 \end{bmatrix}. \tag{2}$$

Furthermore, the matrix E can be diagonalized as

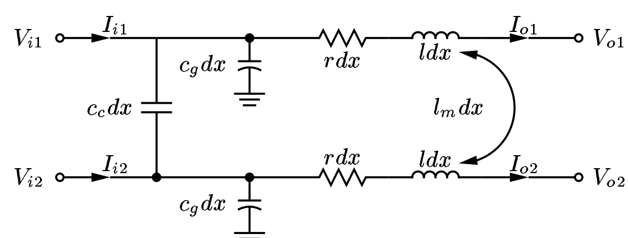

Fig. 1. Infinitesimally small segment of two coupled identical *RLC* interconnects

This research is supported in part by the Semiconductor Research Corporation under Contract No. 2003-TJ-1068, the DARPA/ITO under AFRL Contract F29601-00-K-0182, the National Science Foundation under contract No. CCR-0304574, the Fulbright Program under grant # 87481764, grants from the New York State Office of Science, Technology & Academic Research to the Center for Advanced Technology - Electronic Imaging Systems and to the Microelectronics Design Center, and by grants from Xerox Corporation, IBM Corporation, Intel Corporation, Lucent Technologies Corporation, and Eastman Kodak Company.

$$E^n = \frac{1}{2}\begin{bmatrix} \cosh(h\theta_1)+\cosh(h\theta_2) & \cosh(h\theta_1)-\cosh(h\theta_2) & Z_{o1}\sinh(h\theta_1)+Z_{o2}\sinh(h\theta_2) & Z_{o1}\sinh(h\theta_1)-Z_{o2}\sinh(h\theta_2) \\ \cosh(h\theta_1)-\cosh(h\theta_2) & \cosh(h\theta_1)+cosh(h\theta_2) & Z_{o1}\sinh(h\theta_1)-Z_{o2}\sinh(h\theta_2) & Z_{o1}\sinh(h\theta_1)+Z_{o2}\sinh(h\theta_2) \\ \frac{\sinh(h\theta_1)}{Z_{o1}}+\frac{\sinh(h\theta_2)}{Z_{o2}} & \frac{\sinh(h\theta_1)}{Z_{o1}}-\frac{\sinh(h\theta_2)}{Z_{o2}} & \cosh(h\theta_1)+\cosh(h\theta_2) & \cosh(h\theta_1)-\cosh(h\theta_2) \\ \frac{\sinh(h\theta_1)}{Z_{o1}}-\frac{\sinh(h\theta_2)}{Z_{o2}} & \frac{\sinh(h\theta_1)}{Z_{o1}}+\frac{\sinh(h\theta_2)}{Z_{o2}} & \cosh(h\theta_1)-\cosh(h\theta_2) & \cosh(h\theta_1)+\cosh(h\theta_2) \end{bmatrix} \quad (12)$$

$$E = W\Lambda W^{-1}, \quad (3)$$

where

$$\Lambda = \begin{bmatrix} (1-\theta_1 dx) & 0 & 0 & 0 \\ 0 & (1+\theta_1 dx) & 0 & 0 \\ 0 & 0 & (1-\theta_2 dx) & 0 \\ 0 & 0 & 0 & (1-\theta_2 dx) \end{bmatrix}, \quad (4)$$

$$W = \frac{1}{2}\begin{bmatrix} -Z_{o1} & Z_{o1} & Z_{o2} & -Z_{o2} \\ -Z_{o1} & Z_{o1} & -Z_{o2} & Z_{o2} \\ 1 & 1 & -1 & -1 \\ 1 & 1 & 1 & 1 \end{bmatrix}, \quad (5)$$

and

$$dx = \frac{h}{n}, \quad (6)$$

$$\theta_1 = \sqrt{sC_g(r+s(l+l_m))}, \quad (7)$$

$$\theta_2 = \sqrt{s(C_g+2C_c)(r+s(l-l_m))}, \quad (8)$$

$$Z_{o1} = \sqrt{\frac{(r+s(l+l_m))}{sC_g}}, \quad (9)$$

$$Z_{o2} = \sqrt{\frac{(r+s(l-l_m))}{s(C_g+2C_c)}}. \quad (10)$$

The physical meaning of θ_1 (Z_{o1}) is the propagation constant (characteristic impedance) of coupled interconnects when both inputs switch in the same direction. The physical meaning of θ_2 (Z_{o2}) is the propagation constant (characteristic impedance) of coupled interconnects when both inputs switch in opposite directions.

Using $dx = \frac{h}{n}$, $E^n = (W\Lambda W^{-1})^n = (W\Lambda^n W^{-1})$, and the identity,

$$\lim_{n\to\infty}(1+\frac{x}{n})^n = e^x, \quad (11)$$

E^n can be obtained as shown in (12). For the driver and receiver ends of two identical coupled *RLC* interconnects,the ABCD matrices are

$$E^i = \begin{bmatrix} 1 & 0 & R_s & 0 \\ 0 & 1 & 0 & R_s \\ 0 & 0 & 1 & 0 \\ 0 & 0 & 0 & 1 \end{bmatrix}, \quad (13)$$

$$E^o = \begin{bmatrix} 1 & 0 & 0 & 0 \\ 0 & 1 & 0 & 0 \\ sC_L & 0 & 1 & 0 \\ 0 & sC_L & 0 & 1 \end{bmatrix}. \quad (14)$$

By solving the *Kirchhoff* equation for coupled interconnects,

$$\Psi_i = E^i E^n E^o \Psi_o, \quad (15)$$

the output voltages $V_{o1}(s)$ and $V_{o2}(s)$ of these two coupled interconnects can be obtained as

$$\begin{bmatrix} V_{o1}(s) \\ V_{o2}(s) \end{bmatrix} = \frac{1}{2}\begin{bmatrix} H_1(s)+H_2(s) & H_1(s)-H_2(s) \\ H_1(s)-H_2(s) & H_1(s)+H_2(s) \end{bmatrix}\begin{bmatrix} V_{i1}(s) \\ V_{i2}(s) \end{bmatrix}, \quad (16)$$

where

$$H_1(s) = \frac{1}{(1+sR_sC_L)cosh(\theta_1 h)+(\frac{R_s}{Z_{o1}}+sC_L Z_{o1})sinh(\theta_1 h)}, \quad (17)$$

$$H_2(s) = \frac{1}{(1+sR_sC_L)cosh(\theta_2 h)+(\frac{R_s}{Z_{o2}}+sC_L Z_{o2})sinh(\theta_2 h)}. \quad (18)$$

Note that $H_1(s)$ and $H_2(s)$ are in the same format as the transfer function of a single transmission line [1]. The output voltages of two coupled interconnects can, therefore, be determined from (16) using the transfer functions of the two independent interconnect systems, $H_1(s)$ and $H_2(s)$. When the input of the victim line is at ground, the coupling noise caused by the aggressor $V_{agg}(s)$ is

$$V_{noise}(s) = \frac{1}{2}(H_1(s)-H_2(s))V_{agg}(s) \quad (19)$$

$$= \frac{1}{2}(\overline{V}_{o1}(s)-\overline{V}_{o2}(s)). \quad (20)$$

The decoupled interconnects are shown in Fig. 2.

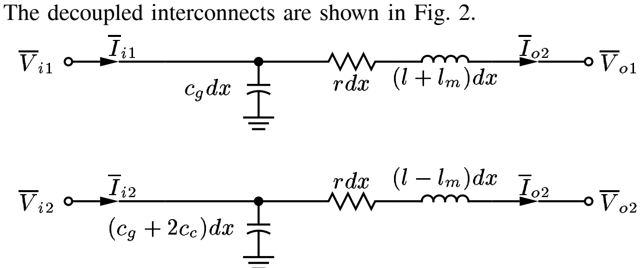

Fig. 2. Infinitesimally small segment of decoupled interconnects

III. Peak Noise of Two Coupled Interconnects

For the coupled interconnects shown in Fig. 1, the transient response at the two outputs can be expressed using the normalized variables listed in Table I [7]. Furthermore, in order to characterize the effect of inductance on the crosstalk noise, a parameter ζ, described in [8], is used, where ζ is defined as

$$\zeta = \frac{R_T + R_T C_T + R_R C_T + 0.5R_R}{2\sqrt{(1+C_T)}}. \quad (21)$$

The crosstalk noise can therefore be expressed using only five variables, ζ, C_T, R_T, K_C, and K_L.

The decoupled interconnects shown in Fig. 2 can be used to determine the peak crosstalk noise. For two strongly inductively coupled interconnects ($K_L \gg K_C$ such that $t_{f1} > t_{f2}$), the waveform of the coupling noise and the output waveforms, $\overline{V}_{o1}(t)$ and $\overline{V}_{o2}(t)$, of the decoupled interconnects are shown in Fig. 3, where t_{f1} and t_{f2} are

$$t_{f1} = h\sqrt{(l+l_m)c_g}, \quad (22)$$

$$t_{f2} = h\sqrt{(l-l_m)(c_g+2c_c)}. \quad (23)$$

t_{f1} and t_{f2} are the time of flight of two decoupled interconnects, respectively.

As expressed in (20), the waveform of the coupling noise can be determined by subtracting the decoupled voltage $\overline{V}_{o2}(t)$ from $\overline{V}_{o1}(t)$.

TABLE I
NORMALIZED VARIABLES FOR TWO COUPLED INTERCONNECTS

Variable	Definition	Physical Meaning
Z_o	$\sqrt{l/c_g}$	Characteristic impedance
t_f	$h\sqrt{lc_g}$	Time of flight
R_R	hr/Z_o	Normalized line resistance
R_T	R_s/Z_o	Normalized driver resistance
C_T	$C_L/(hc_g)$	Normalized load capacitance
K_C	c_c/c_g	Normalized coupling capacitance
K_L	l_m/l	Normalized coupling inductance

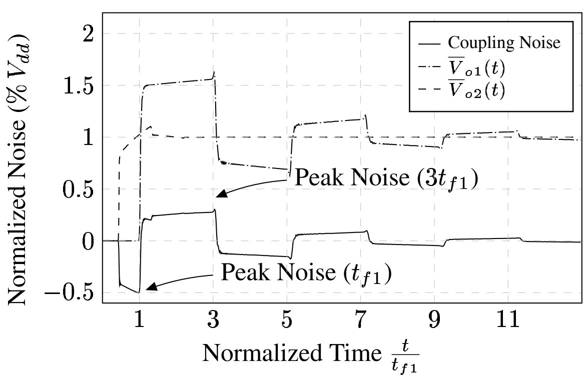

Fig. 3. Output waveform of decoupled interconnects and waveform of coupled noise between two coupled interconnects when $t_{f1} > t_{f2}$ ($K_L = 0.769$ and $K_C = 0.217$). The input of the victim line remains at ground while the input of the aggressor line is a step input.

The negative peak of the coupling noise, therefore, occurs at time t_{f1}, as shown in Fig. 3, and is

$$V_{noise}(t_{f1}) = -\frac{1}{2}\overline{V}_{o2}(t_{f1})\,. \tag{24}$$

At the time of $3t_{f1}$, the decoupled voltage $\overline{V}_{o1}(t)$ is maximum. The positive peak of the coupling noise is

$$V_{noise}(3t_{f1}) = \frac{1}{2}(\overline{V}_{o1}(3t_{f1}) - \overline{V}_{o2}(3t_{f1}))\,. \tag{25}$$

Combining (24) and (25), the peak crosstalk noise of two strongly inductively coupled interconnects is

$$V_{peak} = max\{V_{noise}(t_{f1}), V_{noise}(3t_{f1})\}\,. \tag{26}$$

An analysis of the crosstalk noise when $t_{f1} < t_{f2}$ is similar to an analysis of the crosstalk noise with the positive and negative peak noise occurring at t_{f2} and $3t_{f2}$, respectively. The peak crosstalk noise between two coupled interconnects (either $t_{f1} > t_{f2}$ or $t_{f1} < t_{f2}$) can be unified and is

$$t_{fmax} = max\{t_{f1}, t_{f2})\}, \tag{27}$$
$$V_{peak} = max\{V_{noise}(t_{fmax}), V_{noise}(3t_{fmax})\}. \tag{28}$$

The peak noise in (28) is determined from the transient response of the two decoupled interconnects. In order to determine the precise value of the decoupled voltages $\overline{V}_{o1}(t)$ and $\overline{V}_{o2}(t)$ at t_{fmax} and $3t_{famx}$, a traveling wave based approximation technique (TWA), as described in [9], is used to construct the transient output response of the two decoupled interconnects. In the TWA technique, the low frequency characteristics of the transient signal is represented by a three pole approximation. The high frequency characteristics of the transient signal is determined by the traveling wave characteristics and a modified approximation of the *RC* response.

Based on the TWA technique, the peak crosstalk noise is obtained from (28) and compared to SPICE for various values of the five variables, ζ, C_T, R_T, K_C, and K_L, as shown in Figs. 4,5, respectively (the figures for C_T, R_T, and K_L are omitted to due to space limit). The crosstalk noise model by Davis [4] is also shown in Fig. 4 for comparison. In [4], the crosstalk is assumed to occur at the time of flight t_f.

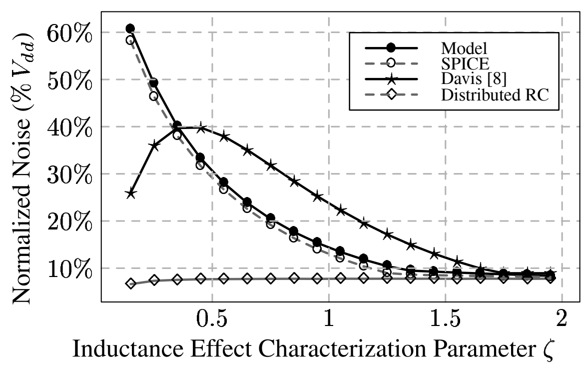

Fig. 4. Comparison of crosstalk model to SPICE, Davis [4], and distributed *RC* model for different values of ζ. ($K_C = 0.217$, $K_L = 0.769$, $C_T = 0.05$, and $R_T = 0.25$)

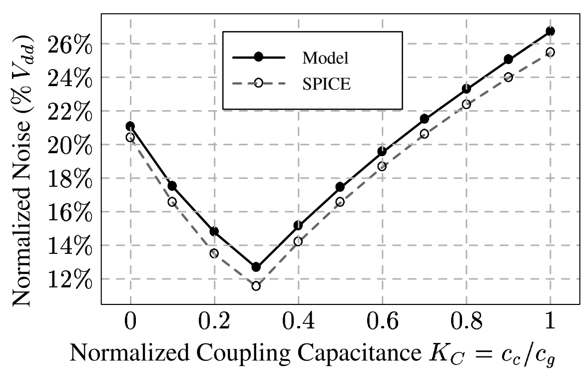

Fig. 5. Comparison of crosstalk model to SPICE for different values of K_C. ($K_L = 0.769$, $\zeta = 1$, $C_T = 0.05$, and $R_T = 0.25$)

The peak crosstalk noise of two coupled *RLC* interconnects decreases when the inductance effect characterization parameter ζ increases (a smaller inductance effect), as shown in Fig. 4. As expected, the distributed *RC* interconnect model can be used to determine the peak crosstalk noise when ζ is sufficient large ($\zeta > 1.5$). The peak noise is almost constant for the normalized load capacitance C_T varying over the practical range of $0 < C_T \leq 0.1$, and decreases with increasing normalized driver resistance R_T. The peak crosstalk noise does not increase monotonically with an increase in the normalized inductive or capacitive coupling factor K_L and K_C, as shown in Fig. 5. The lowest value of the peak crosstalk noise occurs when

$t_{f1} = t_{f2}$, where the waves of two decoupled interconnects $\overline{V}_{o1}$ and $\overline{V}_{o2}$ simultaneously arrive at the receiver end.

Combining (22) and (23) with $t_{f1} = t_{f2}$, the lowest crosstalk noise occurs when the normalized coupling inductance K_L and normalized coupling capacitance K_C satisfy

$$K_C = \frac{K_L}{1 - K_L}. \tag{29}$$

The peak crosstalk noise increases when K_L or K_C deviates from the values that satisfy (29). This peak crosstalk noise model exhibits an average error of 6.8% as compared to SPICE.

IV. Upper limit of peak crosstalk noise between two non-identical coupled interconnects

In Sections II and III, the decoupling technique and a model of the peak crosstalk noise are developed for two identical coupled interconnects. For non-identical coupled interconnects, no analytic decoupling technique exists, therefore, the peak crosstalk noise model cannot be developed in the same manner as described in Section III. The upper limit on the peak crosstalk noise, however, can be obtained for two non-identical coupled interconnects by exploiting physical insight acquired from applying the decoupling technique to two identical coupled interconnects.

Similar to the decoupling technique for two identical coupled interconnects, two non-identical coupled *RLC* interconnects with driver resistances R_{s1} and R_{s2} and load capacitances C_{L1} and C_{L2} are decoupled by calculating the effective inductances and capacitances for both inputs switching in the same and opposite directions, as shown in Fig. 6. When both inputs switch in the same direction, the aggressor line (l_1, c_1) sees an effective inductance of $l_1 + l_m$ and an effective capacitance of c_{g1}, respectively. When both inputs switch in opposite directions, the victim line (l_2, c_2) sees an effective inductance of $l_2 - l_m$ and an effective capacitance of $c_{g2} + 2c_c$, respectively.

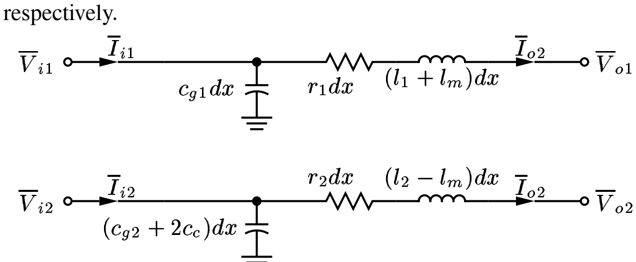

Fig. 6. Infinitesimally small segment of decoupled interconnects. Note that this decoupled circuit is used to determine the upper limit rather than the peak crosstalk noise.

Note that this decoupled circuit is used to determine the upper limit rather than the peak crosstalk noise. The upper limit can be obtained from (28) by using the decoupled circuit shown in Fig. 6. A comparison of the upper limit of the peak crosstalk noise with SPICE for different values of C_1 and C_2 is shown in Figs. 7.

V. Conclusions

Based on the ABCD parameter matrix, a decoupling technique for two identical coupled *RLC* interconnects is presented. The inductances (capacitances) of the two decoupled interconnects are the effective inductances (capacitances) when both inputs switch in the same and opposite directions, respectively. A model of the peak crosstalk noise is developed based on this decoupling technique, with the peak noise occurring at the time of flight t_{fmax} or $3t_{fmax}$. The model exhibits an average error of 6.8% as compared to SPICE. The peak crosstalk noise decreases with an increase in the inductance effect characterization parameter ζ. A distributed *RC* model of the interconnects can be used to determined the crosstalk noise if ζ is sufficient large ($\zeta > 1.5$). The peak crosstalk noise does not necessarily increase with greater coupling inductance or capacitance. The decoupling technique is further extended to two non-identical coupled interconnects, and an upper limit on the peak crosstalk noise is determined.

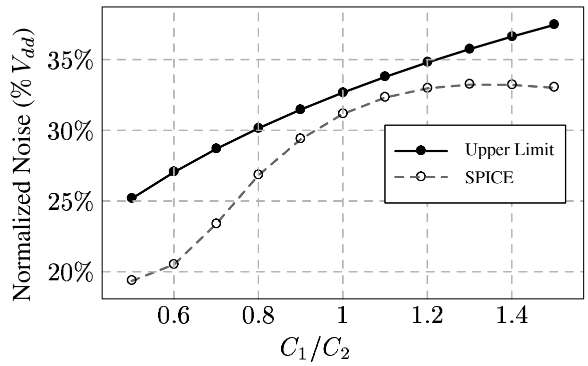

Fig. 7. Comparison of peak crosstalk noise using SPICE with the model for C_1/C_2 varying from 0.5 to 1.5. (C_2 = 1 pF, $L_1 = L_2$ = 6.67 nH, $R_{11} = R_{22}$ = 53.6 Ω, $R_{s1} = R_{s2}$ = 11 Ω, $C_{L1} = C_{L2}$ = 0.05 pF, and h = 5000 μm)

References

[1] K. Banerjee and A. Mehrotra, "Analysis of On-Chip Inductance Effects for Distributed RLC Interconnects," *IEEE Transactions on Computer-Aided Design of Integrated Circuits and Systems*, Vol. 21, No. 8, pp. 904–915, August 2002.

[2] K. T. Tang and E. G. Friedman, "Peak Crosstalk Noise Estimation in CMOS VLSI Circuits," *Proceedings of the IEEE International Conference on Electronics, Circuits and Systems*, pp. 1539–1542, September 1999.

[3] Y. Cao, X. Huang, D. Sylvester, N. Chang, and C. Hu, "A New Analytical Delay and Noise Model for On-Chip RLC Interconnect," *Proceedings of the IEEE International Electron Devices Meeting*, pp. 823–826, December 2000.

[4] A. J. Davis and D. J. Meindl, "Compact Distributed RLC interconnect Models-Part II: Coupled Line Transient Expressions and Peak Crosstalk in Multilevel Networks," *IEEE Transactions on Electron Devices*, Vol. 47, No. 11, pp. 2078–2087, November 2000.

[5] J. Chen and L. He, "A Decoupling Method for Analysis of Coupled RLC Interconnects," *Proceedings of the ACM Great Lakes Symposium on VLSI*, pp. 41–46, April 2002.

[6] W. Jin, S. Yoon, and J. Kim, "Experimental Characterization and Modeling of Transmission Line Effects for High-Speed VLSI Circuit Interconnects," *Institute of Electonics, Information and Communication Engineers Transactions on Electronics*, Vol. 83, No. 5, pp. 728–735, May 2000.

[7] R. Venkatesan, J. A. Davis, and J. D. Meindl, "A Physical Model for the Transient Response of Capacitively Loaded Distributed RLC Interconnects," *Proceedings of the IEEE Design Automation Conference*, pp. 763–766, June 2002.

[8] Y. I. Ismail and E. G. Friedman, "Effects of Inductance on the Propagation Delay and Repeater Insertion in VLSI Circuits," *IEEE Transactions on Very Large Scale Integration (VLSI) Systems*, Vol. 8, No. 2, pp. 195–206, April 2000.

[9] Y. Eo, J. Shim, and W. R. Eisenstadt, "A Traveling-Wave-Based Waveform Approximation Technique for the Timing Verification of Single Transmission Lines," *IEEE Transactions on Computer-Aided Design of Integrated Circuits and Systems*, Vol. 21, No. 6, pp. 723–730, June 2002.